Characteristics of T (0, 1) Guided-wave Point-Focusing Electromagnetic Acoustic Transducer for Pipe Inspection

Songling Huang, *Senior Member, IEEE,* Hongyu Sun, Gongtian Shen, Baoxuan Wang, Qing Wang, *Senior Member, IEEE,* Jun Zou and Shen Wang

***Abstract*—Electromagnetic acoustic transducers (EMATs) are widely used in the field of non-destructive testing (NDT) and non-destructive evaluation (NDE) due to their advantages of non-contact and applicability in complex environments. However, their low energy-conversion efficiency restricts their application in industrial testing. This work proposes a newly designed focusing EMAT based on the T (0, 1)-wave in a pipe to improve the energy conversion efficiency of EMATs. The focal length and defect width are investigated in this paper, and the advantages of the newly designed point-focusing transducer are shown in comparison with traditional unfocused transducers. Results show that the newly designed pipe focusing EMAT can increase the intensity of the defect reflection wave by around 60%, and the reflected wave intensity can be enhanced by 70% in the experiment when compared to the unfocused one.**

***Index Terms*— T (0,1) guided-wave, point-focusing, periodic permanent magnet, focal length, defect width.**

I. Introduction

Non-destructive testing (NDT) technology is a method of determining the physical properties, state, and internal structure of the material without damaging it [1-5]. The primary means of NDT include: ultrasonic testing [6], magnetic flux leakage testing [7], eddy current testing [8], radiation testing in medical treatment [9], and optical fiber for long-term strain detection for buildings [10]. Among these methods, ultrasonic testing, particularly with guided-wave technology, is widely used in industrial testing to detect defects in thin-walled plates and pipes [11-13]. As a sound detection technology, ultrasonic guided-waves can travel very far along a pipe with little attenuation, and offer a clear directionality in the propagation process, so that defects in the specimen at various positions along the guided-wave propagation path can be detected [14]. Among ultrasonic wave generation methods, piezoelectric transducers that can excite sound waves in a specimen are currently widely used [15]. However, this method requires grinding of the contact surface and a couplant. Therefore, it is unsuitable for complicated detection of environmental conditions such as high temperature. Accordingly, an electromagnetic acoustic transducer (EMAT) can replace the traditional piezoelectric transducer as a method of generating electromagnetic ultrasonic guided-waves without a couplant [16]. However, its main drawback, namely its low energy-conversion efficiency, makes it challenging to apply in industrial testing.

Therefore, to solve this problem of the low energy-conversion efficiency, it is necessary to exhibit specific methods that can analyze the physical phenomenon of the EMAT and waves. The wave structure and dispersion curves can describe the characteristics of the guided-waves in most studies while the velocity-frequency relationship can be used to select the wave mode with a non-dispersive feature [17]. When studying the ultrasonic wave field in a specimen, displacement of the whole domain or a certain point is always shown to describe the vibration, transmission, and reflection processes of sound waves as they encounter defects [18]. Therefore, the working characteristics of various transducers and the transmission process of guided-waves can be obtained by analyzing the wave structure.

An axially uniformly distributed transducer array is widely used to generate an axisymmetric axial ultrasonic guided-wave, and such a guided-wave can enable rapid detection of a pipe [19, 20]. However, this method is insufficient for detecting small defects on a pipe wall, and cannot determine the circumferential position of any defect. To solve this problem and increase the intensity of the detection signal, a method of ultrasonic body waves to detect pipe defects has been proposed with the use of shear-vertical (SV) waves [21]. Although this method can enable the focusing of the ultrasonic waves and can detect pipe surface defects, such transducers still require mechanical movement on the surface of the pipe to achieve full inspection, which is difficult to perform in long-distance pipe inspection. In the field of focusing guided-waves in a pipe, a natural beam focusing by exciting non-axisymmetric Lamb waves was proposed with the use of the frequency and excitation adjustment method [22]. However, this method can only achieve natural focusing under ideal conditions, and the zero-displacement point that exists periodically along the pipe is not conducive to the detection of defects. Another

*Correspondence to: Shen Wang. (Email: wangshen@mail.tsinghua.edu.cn)
State Key of Power Systems, Department of Electrical Engineering, Tsinghua University, Beijing, 10084, China
Songling Huang, Hongyu Sun, andJun Zhou are with the State Key Laboratory of Power System, Department of Electrical Engineering, Tsinghua University, Beijing 100084, China
Q. Wang is with the Department of Engineering, Durham University, Durham DH1 3LE, U.K.
Gongtian Shen, Baoxuan Wang are with the China Special Equipment Inspection and Research Institute, Beijing, 100029, China

method of focusing ultrasonic waves is phased array focusing, and an axial guided-wave focusing method is implemented [23].

Moreover, the corresponding simulation and experiment also proved the feasibility of the phased array guided-wave focusing method in the studies [24， 25]. However, such phased array transducers require precise computer programming, and multiple transducers are required for phase control, so the implementation of this focusing method is both complicated and expensive. In a previous study, we proposed a focusing EMAT with the use of SH-0 waves to inspect defects on a plate [26]. Besides, the T(0, 1) wave of a pipe can be converted into the SH-0 wave of an unwrapped plate when the pipe radius is much larger than the wall thickness, [27, 28]. Specifically, these similarities including the dispersion curves and displacement distributions between the pipe and plate guided-waves can be used to focus the waves in a pipe using a fan-shaped periodic permanent magnet (PPM) focusing EMAT.

Here, we propose a new guided-wave point-focusing EMAT with a fan-shaped PPM that is suitable for inspecting pipe defects, and racetrack-like coils with burst current are used to generate focusing T(0, 1) guided-waves. For comparison with the focusing EMAT, the traditional unfocused parallel coil EMAT has also been studied. The influences of different focal lengths and defect widths on the reflected wave signals from the defect are studied.

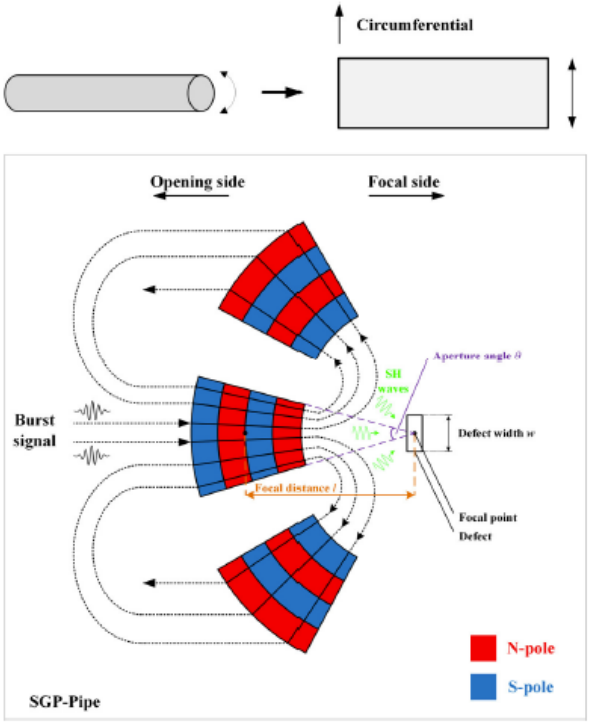

Fig. 1 2-D schematic diagram of a new designed T(0,1) guided wave point-focusing EMAT, the EMAT sensor locates outside the pipe wall

II. Model Description

To study the newly designed point-focusing EMAT with PPM, geometric and physical models are proposed to describe the configuration of the structure in detail. The simulation is implemented using the Finite Element Method (FEM), and the methods are also introduced in the following sections.

A. Geometric model

To achieve the ultrasonic guided-wave focusing of a pipe, it is necessary to reasonably design the EMAT's structure: coil arrangement and permanent magnet setting. The wall thickness of the pipe is much smaller than its radius, and the T (0, 1)-wave has the same dispersion curves and wave structures as the SH0-wave mode [29]. The design method of the focusing transducer can be therefore related to our previous studies on plate focusing [30, 31], while necessary changes must be made for a pipe. Fig. 1 shows the schematic diagram of coils and the fan-shaped PPM. Burst signals with 1 MHz center frequency and 2 A current amplitude are applied on the coils, which are placed as a fan shape to achieve the point-focusing capability of a transducer. The focal length l is defined as the focal radius of coils, and the focal point is selected at the defect center. In this work, the defect length (axial direction) and depth keep unchanged while the defect width (circumferential direction) varies in order to study the effect of defect size. The EMAT with racetrack-like coils is utilized to ensure the wave focusing [32], and the PPM with S-N-S-N arrangement is placed at the center, while the other two PPMs placed on both sides with the opposite magnetic arrangement (N-S-N-S). This particular arrangement of coil-magnets maintains the emission of the ultrasonic waves consistently, thereby achieving phase interference and directional focusing of guided-waves at a predetermined focal point.

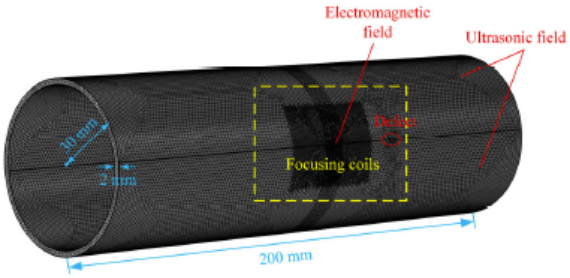

Fig. 2 The size, physical fields, and mesh distribution of the simulation model.

B. Physical model

The generation and propagation process of guided-waves in a pipe can generally be described by the electromagnetic field and ultrasonic field. The ultrasonic wave, as an elastic wave, is generated by an induced eddy in a conductor and propagates within the specimen due to the Lorentz force under the bias magnetic field. The dynamic magnetic field equation of pulsed eddy current is [33-35].

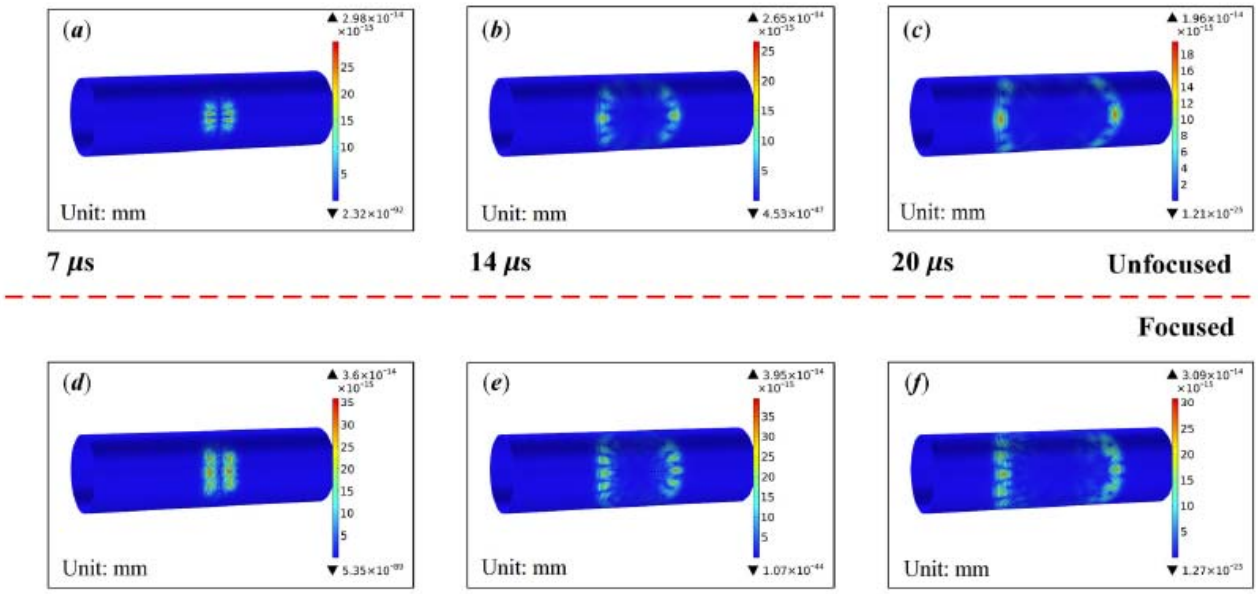

Fig. 3 Wave displacement distribution: (a-c) Unfocused and (d-f) focused EMAT at different moments.

$$\frac{1}{\mu}\nabla^2 A+\frac{1}{S}\iint_s \sigma\frac{\partial A}{\partial t}\mathrm{d}s=\sigma\frac{\partial A}{\partial t}-\frac{i}{S} \quad (1)$$

where **A** is the magnetic vector potential; σ is the conductivity; *i* is the total current; S is the cross-sectional area of the coil conductor. The induced eddy current density is

$$J_e=-\sigma\frac{\partial A}{\partial t} \quad (2)$$

Accordingly, the Lorentz force F generated by the eddy current under the applied bias magnetic field is

$$F_v=J_e\times(B_d+B_s) \quad (3)$$

where $\mathbf{B}_d$ indicates the dynamic magnet flux density; **B**s is the static magnetic flux density of the PPM. It is known that Lorentz force plays a vital role in the interaction of physical fields as a coupling factor. Because the periodic Lorentz force will generate elastic waves propagating in the specimen along a certain direction. The wave equation which equals the Navier's equation of the elastic wave can be expressed as

$$(\lambda+\mu)\nabla\nabla\cdot u=\rho\frac{\partial^2 u}{\partial t^2}-\mu\nabla^2 u-F_v \quad (4)$$

where u represents the displacement vector; Fv is the calculated Lorenz force in the electromagnetic field model; λ and μ are the Lame's constants of the material. Eq. (4) shows that the displacement in the specimen varies with time under Lorentz forces, which describes the propagation process of elastic waves.

Therefore, to describe the propagation characteristics of the guided-wave in a pipe, the electromagnetic field and ultrasonic field are selected in COMSOL software and used in the simulation. The size, physical fields, and mesh distribution of the simulation model are shown in Fig. 2. Besides, the mesh around the coils and PPM is refined to ensure the accuracy of the eddy current calculation. In the simulation, to improve the calculation efficiency, the electromagnetic field is limited to the vicinity of coils and PPM. The ultrasonic field is applied to the entire calculation domain to describe the wave propagation process. Moreover, the length of the steel pipe is 200 mm, the thickness is 2 mm, and the outer radius is 30 mm. Since the radius is much larger than the wall thickness of the pipe (about 15 times), the circumferential displacement can be approximated as a constant, just like the SH0-wave, thus satisfying the pipe-plate approximation.

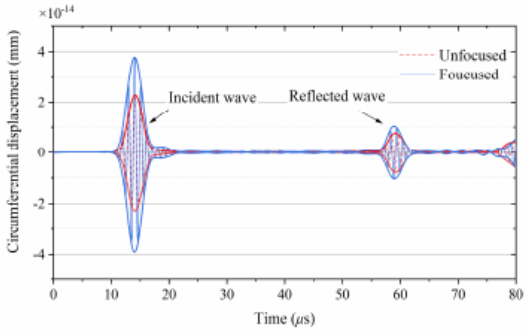

Fig. 4 Circumferential displacement at the focal point for focused and unfocused EMATs.

III. Results

To obtain the characteristics of focusing T (0, 1) mode pipe-waves, the drive frequency of the burst signal is set to 1MHz in accordance with the dispersion curves and our previous study [30], and corresponding simulations have been done. The lift-off distance is set to 1 mm in both simulation and experiment, the remanence magnetism of the PPM is 1.21 T and the focal length is 30 mm. An unfocused

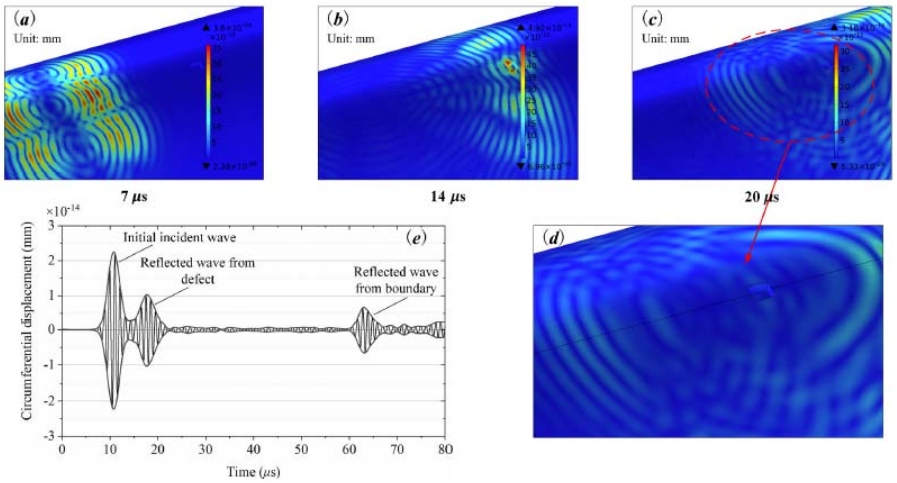

Figure 5 Wave displacement for the palte with a defect: (a-c) Wave propagation reflected by a defect. (d) Partial magnified view of the red dashed circle in (c). (e) The relationship between circumferential displacement and time.

Parallel coil EMAT is used as a comparison of a focused one. Figs. 3(a-c) show the wave displacement distributions of the unfocused EMAT at 7 μs, 14 μs, and 20 μs. It can be seen that guided-waves propagate along both sides, with a peak displacement of 2.65×10-14 mm (at 14 μs). For the focusing EMAT, Figs. 3(d-f) have a peak displacement of 3.95×10-14 mm (at 14 μs) under the same conditions except for the coil arrangement. It shows that the focused EMAT has a larger amplitude at the focal moment. To observe the time-displacement variation at the focal point of the two EMATs, Fig. 4 shows the circumferential displacement at this point for both focused and unfocused EMATs that demonstrated in Fig. 3. It shows that the initial wave arrives at around 10 μs and then reaches its peak at 14 μs. The second wave is the reflected wave from the pipe's boundary, which is much smaller than the initial one. In the simulation, compared with the traditional parallel unfocused EMAT, the new pipe focusing method can increase the wave signal at the focal point by 49%. It illustrates that the wave intensity of the focused EMAT is higher than that of the unfocused EMAT when there is no defect in the specimen.

Since the pipe EMAT is used to detect defects, further research on the defective pipe is required. In the simulation, the focal length is 30 mm, and the defect position is on the central axis of the transducer. For the size of the defect, its length (axial direction) and depth (radial direction) are fixed to 1 mm, and the width (circumferential direction) is set to 2 mm in the simulation. Figs. 5(a-c) show the wave propagation and defect reflected waves for the focusing EMAT at 7 μs, 14 μs, and 20 μs, respectively. In addition, Fig. 5(d) is a partial magnified view of the dashed circle in Fig. 5(c). Due to the presence of the defect, part of the waves is transmitted to the other side, and others propagate in the opposite direction because of reflection. To measure the reflected waves, a receiving transducer with parallel arrayed PPM is placed 10 mm away from the defect, and it converts the received displacement signal into the voltage signal. However, in the simulation, the circumferential displacement at the measuring point can be obtained directly without the signal conversion process. Fig. 5(e) shows the relationship between the circumferential displacement and time. The initial incident waves, reflected waves from the defect, and reflected waves from the boundary can be seen in this figure. It shows that the reflected wave has a certain attenuation compared with the initial incident wave, and its amplitude can be obtained. Therefore, through the above methods and results, the effects of different focal lengths and different defect widths on the newly designed point-focusing guided-wave EMAT can be investigated.

IV. Discussions

A. Effect of the focal length

Although wave focusing improves upon the signal-to-noise ratio (SNR) of the defect detection signal, a suitable focal length selection is also very important. A focal length that is too small is not conducive to effectively detect defects, and a large length may lead to low focal signal intensity, thus affecting the detection process. Since the ultrasonic wave gradually decays during the propagation process, the focal length is one of the main factors affecting the efficiency of the transducer. Therefore, the effect of focal length on the focusing EMAT performance is required to be studied.

In this work, the defect size keeps unchanged with a 2 mm width, while its position changes as the focal length increases. Five focal lengths (30 mm, 40 mm, 50 mm, 60 mm, 70 mm) are selected while the measuring point remains the same. Fig. 6(a) shows the positional relationship between focusing coils, measure point and defects (also refer to the focal point). In Figs. 6(b-f), wave signals at the measuring point under various focal lengths are shown, and Fig. 7 shows the normalized

amplitude of reflected waves. It can be found that as the focal length increases, the reflected wave signal gradually decreases, and this attenuation is non-linear: The initial decrease is very fast, and as the focal length continues to increase, the changing rate of the signal amplitude gradually decreases. As the focal length increases, the reflected wave intensity of the focused EMAT will be reduced by 90%.

For the unfocused EMAT in the same position, the reflected wave intensity is lower, which is reduced by about 40%. When the focal length is extended to 40 mm, the signal intensity is reduced by 60%; when the focal length is extended to 50 mm, the signal intensity is further reduced by 80%. Although focusing EMAT can improve the intensity of reflected signals, for larger focal lengths, there may still be problems in the defect detection. Therefore, a shortening of the focal length will help to improve the capability of the new pipe focusing transducer. Moreover, compared to traditional transducers, the focusing EMAT has stronger energy focusing capability. Fig. 7 shows that the newly designed pipe focusing transducer can increase the non-focused EMAT's reflection wave intensity by around 60%。

B. Effect of the defect width

Reflection and transmission phenomena of ultrasonic waves occur when the guided-wave encounters the defect, and the intensity of the reflected wave is related to the geometrical size of the defect. Compared with the axial length, the circumferential width of the defect has a more significant influence on the excited ultrasound by the point-focusing EMAT. Therefore, it is necessary to study the focusing capability of the new EMAT under different defect widths (circumferential direction).

In this work, the length (axial direction) and depth (radial direction) of the defect are fixed to 1 mm. Fig. 8(a) shows the contour of the defect, and the axial length represents the wave propagation direction, and the circumferential width represents the vibration direction of the wave. The defect widths are 2 mm, 4 mm, 6 mm in Figs. 8(b-d), and it can be seen in the figure that the amplitude of the reflected waves increases with the defect width. Fig. 9 shows the normalized amplitude of the reflected waves for both focused and unfocused coils EMATs. As the defect width increases, the reflected wave amplitude increases linearly. And the newly designed pipe focusing EMAT enables a higher signal intensity, which is about 60 % higher than the traditional unfocused transducers. Specifically, the amplitude of sound intensity can be increased by 62%, 61%, 64%, 60%, 63% when the defect width is 1-6 mm respectively. This indicates that when the position of the transducer and the measuring point are pre-determined, the defect width is linear with the signal amplitude of reflected waves. Therefore, this feature can be applied in practice to quantify defects, and by using the newly designed pipe focusing transducers, the quantization accuracy and defect-recognition capability can be greatly improved.

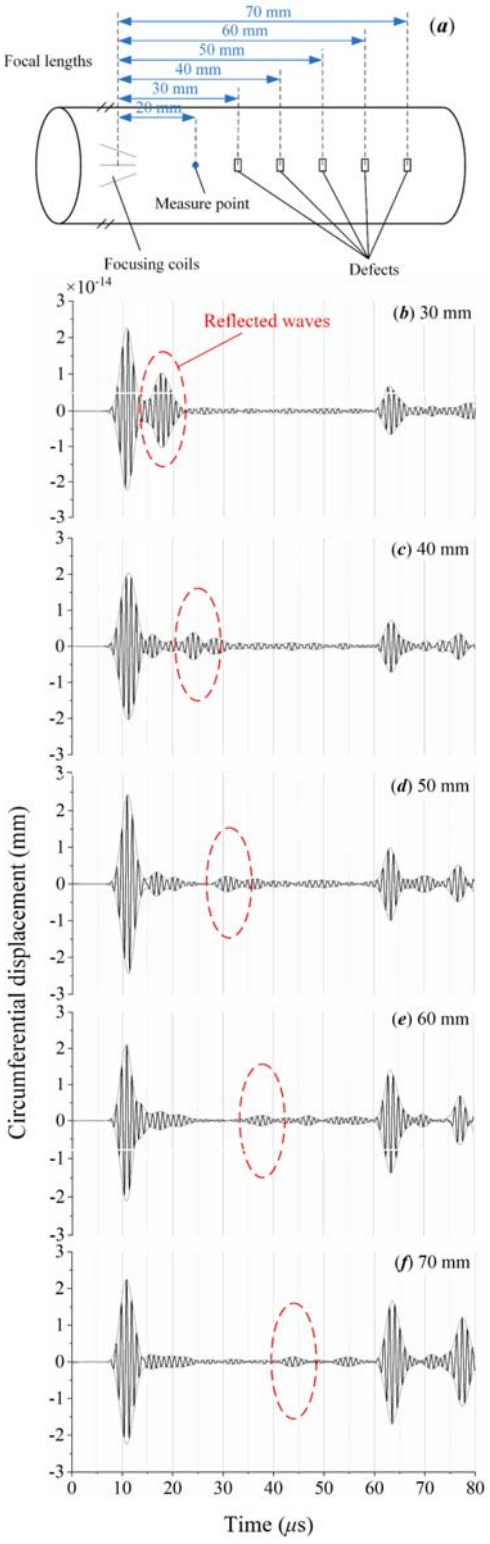

Fig. 6 The effect of the focal length on the signal intensity: (a) positional relationship between focusing coils, measure point and defects; (b-f) wave signals at the measure point under different focal lengths.

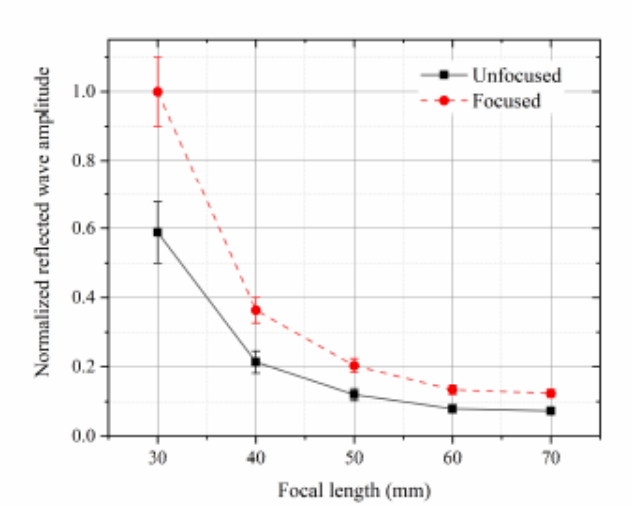

Fig. 7 Normalized reflected wave amplitude at the measure point under different focal lengths for focused and unfocused EMATs.

C. Experimental verification

In this paper, the PPM focusing EMAT is employed to generate a T(0, 1)-wave in the pipe, which can be analogized to the SH-0 guided-wave in a plate. The focusing coils offer a 0.5 mm width with an aperture angle θ of 30 °, and has 20 turns in the experiment. The PPM has a thickness of 6 mm and its remanence magnetism is 1.21 T. The spacings of the PPM array is 1.6 mm, which equals to the half wavelength of the T(0, 1)-wave at a frequency of 1 MHz; thus the ultrasonic phase superposition can be achieved.

As shown in Fig. 10, the experimental system is realized by a newly designed fan-shaped PPM focusing EMAT transmitting system, and an arrayed PPM EMAT receiving system. The pipe used in the experiment is also shown in this figure. The pulses power (RPR 4000) is used as a power source, generating the 1 MHz burst signal to the coils. The signal can be amplified by a power amplifier, which can increase the intensity of the generated signal. Moreover, impedance matching is achieved by placing the resistor in parallel with the coil.

The receiving system is placed at the measuring point, as depicted in the simulation, which is 10 mm away from the defect. From the experimental results, the voltage signal of the array PPM EMAT can be obtained. The measured signal is visualized on the oscilloscope and PC through impedance matching and amplifier (provides filtering and signal amplification).

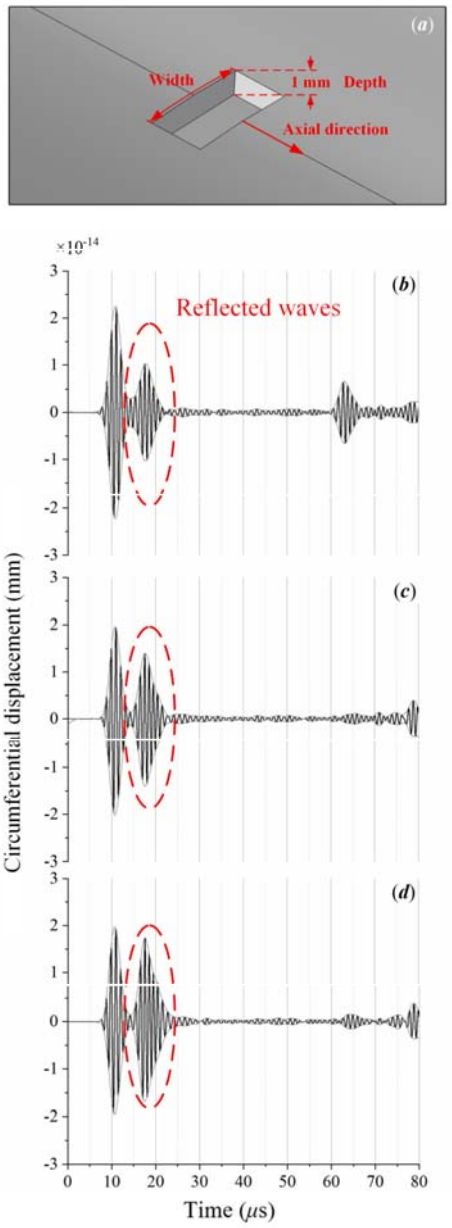

Fig. 8 The effect of the defect width on the signal intensity: (a) the contour of the defect; (b-d) the amplitude of the reflected waves under different defect width.

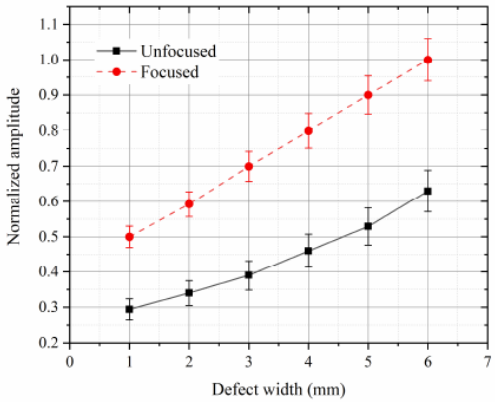

Fig. 9 Normalized reflected wave amplitude at the measure point under different defect widths for focused and unfocused EMATs.

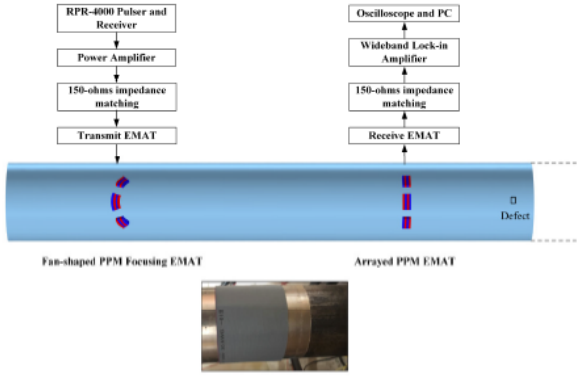

Fig. 10 The experimental system of the newly designed point-focusing EMAT.

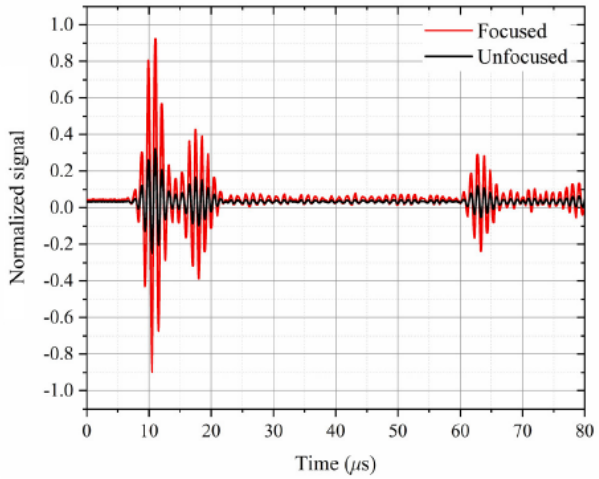

Fig. 11 Experimental results for focused and unfocused EMATs.

In the experiment, the focal length is fixed to 30 mm, and the defect width is 2 mm. Moreover, the steel pipe length is 200 mm, the thickness is 2 mm and the outer radius is 30 mm. The detected signals of the two EMATs are shown in Fig. 11, where the first pulse is the initial wave, the second one is the reflected wave from the defect, and the third one is the reflected wave from pipe boundary. Compared with Fig. 5(e), it can be found that the normalized values of the two figures are relatively close, and reflected wave signals of the defect can be clearly displayed. As shown in Fig. 11, the reflected wave signal intensity is improved by nearly 70% compared to the non-focused traditional transducer. This also proves the advantages of the newly designed focusing transducer in defect detection.

V. Conclusions

In this work, a newly designed focusing EMAT based on the T(0, 1)-wave in a pipe is proposed using fan-shaped PPM and racetrack-like coils. The traditional unfocused parallel coil EMAT has also been investigated as a comparison of the focusing EMAT. The results show that the focusing EMAT has a higher signal intensity at the focal point when there is no defect on the pipe, and its signal is nearly 50% higher than that of the conventional unfocused EMAT. In addition, when the defect exists, the effects of different focal lengths and defect widths on the reflected wave signals are studied in this paper, and then they are compared with the traditional EMAT.

The results show that the increase in the focal length significantly reduces the reflected wave signal intensity. As the focal length increases, the reflected wave intensity of the focused EMAT will be reduced by 80% when the focal length reaches 50 mm. Moreover, the signal increases linearly as the defect width increases. Moreover, the newly designed pipe focusing EMAT has a higher signal intensity, which is about 60 % higher than the traditional unfocused transducers. In either case, the newly designed pipe focusing EMAT has a higher reflected-wave signal intensity than the traditional unfocused EMAT, which is about 60% in the study. Through the experiment, the sufficient focusing capability of the newly designed EMAT is confirmed, and the signal intensity is increased by nearly 70% compared to unfocused transducers. Both simulated and experimental results show that the newly designed point-focusing EMAT is more sensitive to the detection of pipe defects when compared to the traditional unfocused one.

ACKNOWLEDGMENTS

This research was supported by the National Key R&D Program of China (Grant No. 2018YFF01012802), National Natural Science Foundation of China (NSFC) (Grant No. 51677093 and National Natural Science Foundation of China (NSFC) (No. 51777100).

References

[1] C. B. Thring, Y. Fan and R. S. Edwards, “Multi-coil focused EMAT for characterisation of surface-breaking defects of arbitrary orientation,” NDT&E Int., vol. 88, pp. 1-7, 2017.

[2] S. Wang, S. Huang, Y. Zhang, and W. Zhao, “Multiphysics Modeling of a Lorentz Force-Based Meander Coil Electromagnetic Acoustic Transducer via Steady-State and Transient Analyses,” IEEE Sens. J., vol. 16, pp. 6641-6651, 2016.

[3] S. Legendre, D. Massicotte, J. Goyette, et al, “Neural classification of Lamb wave ultrasonic weld testing signals using wavelet coefficients,” IEEE Trans. Instrum. Meas., vol. 50, no. 3, pp. 672-678, 2001.

[4] S. Legendre, D. Massicotte, J. Goyette, et al, “Wavelet-transform-based method of analysis for Lamb-wave ultrasonic NDE signals,” IEEE Trans. Instrum. Meas., vol. 49, no. 3, pp. 524-530, 2000.

[5] J. Silva, M. Wamzeller, P. Farias and J. Neto, “Development of Circuits for Excitation and Reception in Ultrasonic Transducers for Generation of Guided-waves in Hollow Cylinders for Fouling Detection,” IEEE Trans. Instrum. Meas., vol. 57, no. 6, pp. 1149-1153, 2008.

[6] H. M. Seung, C. I. Park, and Y. Y. Kim, “An omnidirectional shear-horizontal guided wave EMAT for a metallic plate,” Ultrasonics, vol. 69, pp.58–66, 2016.

[7] S. Huang, L. Peng, Q. Wang, S. Wang, and W. Zhao, “An Opening Profile Recognition Method for Magnetic Flux Leakage Signals of Defect,” IEEE T. Instrum. Meas., vol. 68, pp. 2229-2236, 2019.

[8] D. I. Ona, G. Y. Tian, R. Sutthaweekul, and S. M. Naqvi, “Design and optimisation of mutual inductance based pulsed eddy current probe,” Measurement, vol. 144, pp. 402-409, 2019.

[9] M. Friedrich-Rust, K. Wunder, S. Kriener, F. Sotoudeh, S. Richter, J. Bojunga, E. Herrmann, T. Poynard, C. F. Dietrich, J. Vermehren, S. Zeuzem, and C. Sarrazin, “Liver fibrosis in viral hepatitis: noninvasive assessment with acoustic radiation force impulse imaging versus transient elastography,” Radiology, vol. 252, pp. 595-604, 2009.

[10] H. Wang, L. Jiang, P. Xiang, “Improving the durability of optical fiber sensor based on strain transfer analysis. Optical Fiber Technology,” Oti Fib. Tech., vol. 42, no. 1, pp. 97-104, 2018.

[11] M. Clough, M. Fleming, and S. Dixon, “Circumferential guided wave EMAT system for pipe screening using shear horizontal ultrasound,” NDT E Int., vol. 86, pp. 20-27, 2017.

[12] Nurmalia, N. Nakamura, H. Ogi, and M. Hirao, “Detection of shear horizontal guided-waves propagating in aluminum plate with thinning region,” Jpn. J. Appl. Phys., vol. 50, no. 7S, pp.07HC17, 2011.

[13] Y. Zhang, S. Huang, S. Wang, et al, “Direction-controllable electromagnetic acoustic transducer for SH waves in steel plate based on magnetostriction,” Prog. Electromagn. Res. Symp., vol. 50, pp.151-160, 2016.

[14] P. B. Nagy, F. Simonetti and G. Instanes, “Corrosion and erosion monitoring in plates and pipes using constant group velocity Lamb wave inspection,” Ultrasonics, vol. 54, pp. 1832-1841, 2014.

[15] X. Meng and S. Lin, “Analysis of a Cascaded Piezoelectric Ultrasonic Transducer with Three Sets of Piezoelectric Ceramic Stacks,” Sensors-Basel, vol. 19, p. 580, 2019.

[16] R. B. Thompson, “Physical principles of measurements with EMAT transducers,” Phys. Acoust., vol. 19, pp.157–200, 1990.

[17] Y. Yang, Z. K. Peng, W. M. Zhang, G. Meng, and Z. Q. Lang, “Dispersion analysis for broadband guided wave using generalized warblet transform,” J. Sound Vib., vol. 367, pp. 22-36, 2016.

[18] T. Hayashi, C. Tamayama and M. Murase, “Wave structure analysis of guided-waves in a bar with an arbitrary cross-section,” Ultrasonics, vol. 44, pp. 17-24, 2006.

[19] D. C. Gazis, “Three-Dimensional Investigation of the Propagation of Waves in Hollow Circular Cylinders. I. Analytical Foundation,” The Journal of the Acoustical Society of America, vol. 31, pp. 568-573, 1959.

[20] D. C. Gazis, “Three-Dimensional Investigation of the Propagation of Waves in Hollow Circular Cylinders. II. Numerical Results,” The Journal of the Acoustical Society of America, vol. 31, pp. 573-578, 1959.

[21] N. Nakamura, K. Ashida, T. Takishita, H. Ogi, and M. Hirao, “Inspection of stress corrosion cracking in welded stainless steel pipe using point-focusing electromagnetic-acoustic transducer,” NDT&E Int., vol. 83, pp. 88-93, 2016.

[22] J. Li and J. L. Rose, "Natural beam focusing of non-axisymmetric guided-waves in large-diameter pipes," Ultrasonics, vol. 44, pp. 35-45, 2006.

[23] Li Jian, Rose Joseph L. “Angular-profile tuning of guided-waves in hollow cylinders using a circumferential phased array, IEEE Transactions on Ultrasonics, Ferroelectrics, and Frequency Control, vol. 49, no. 12, 1720-1729, 2002.

[24] Mu J., Zhang, L., Rose, J.L. “Defect circumferential sizing by using long range ultrasonic guided wave focusing techniques in pipe,” Nondestructive Testing and Evaluation, vol. 22, no. 4, 239-253, 2007.

[25] Wei Luo, Rose, J.L. “Phased array focusing with guided-waves in a viscoelastic coated hollow cylinder,” Journal of the Acoustical Society of America, vol. 121, no. 4:1945-1955, 2007.

[26] H. Sun, S. Wang, S. Huang, Q. Wang, and W. Zhao, “Point-Focusing of Shear-Horizontal Wave Using Fan-Shaped Periodic Permanent Magnet Focusing Coils EMAT for Plate Inspection,” IEEE Sens. J., vol. 19, pp. 4393-4404, 2019.

[27] K. R. Leonard and M. K. Hinders, “Guided wave helical ultrasonic tomography of pipes,” The Journal of the Acoustical Society of America, vol. 114, pp. 767-774, 2003.

[28] A. Velichko and P. D. Wilcox, “Excitation and scattering of guided-waves: Relationships between solutions for plates and pipes,” The Journal of the Acoustical Society of America, vol. 125, pp. 3623-3631, 2009.

[29] Sun F , Sun Z , Chen Q , et al. “Characteristics of SH0-wave Converted to T(0, 1)-wave Based on a T-shaped Plate Wrapped Around a Pipe,” IEEE Transactions on Ultrasonics Ferroelectrics and Frequency Control, 2018:1-1.

[30] Sun H, Huang S, Wang Q, Wang S, Zhao W, “Improvement of unidirectional focusing periodic permanent magnet shear-horizontal wave electromagnetic acoustic transducer by oblique bias magnetic field,” Sensors and Actuators: A. Physical. vol. 290, 36-47, 2019.

[31] Songling Huang, Hongyu Sun, Qing Wang, Shen Wang, Wei Zhao. “Unidirectional Focusing of Horizontally Polarized Shear Elastic Waves Electromagnetic Acoustic Transducers for Plate Inspection,” Journal of Applied Physics, vol. 125, no. 17, 2019.

[32] X. Song, G. Qiu, “Optimization of a Focusable and Rotatable Shear-Wave Periodic Permanent Magnet Electromagnetic Acoustic Transducers for Plates Inspection,” Sensors, vol. 17, no. 12, pp. 2722, 2017.

[33] R. Dhayalan, K. Balasubramaniam, “A hybrid finite element model for simulation of electromagnetic acoustic transducer (EMAT) based plate waves,” NDT&E International, vol. 43, pp. 519-526, 2010.

[34] R. Jafari-Shapoorabadi, A. Konrad, A. N. Sinclair, “Improved finite element method for EMAT analysis and design,” IEEE Transactions on Magnetics, vol. 37, no. 4, pp. 2821-2823, 2001.

[35] K. Mirkhani, C. Chaggares, C. Masterson, er al., “Optimal design of EMAT transmitters,” NDT&E International, vol. 37, pp. 181-193, 2004.